

## A Generalized Dynamic Model of Geared System: Establishment and Application \*

Hui Liu<sup>1,2†</sup>

*1 School of Mechanical Engineering, Beijing Institute of Technology, Beijing 100081, P. R.China*

*2 Science and Technology on Vehicle Transmission Laboratory, Beijing 100081, P. R.China*

Mingzheng Wang

*School of Mechanical Engineering, Beijing Institute of Technology*

*Beijing, 100081, P.R.China*

Zhongchang Cai

*School of Mechanical Engineering, Beijing Institute of Technology*

*Beijing, 100081, P.R.China*

Received 17 August 2011

Accepted 25 November 2011

### Abstract

In order to make the dynamic characteristic simulation of the ordinary and planetary gears drive more accurate and more efficient, a generalized dynamic model of geared system is established including internal and external mesh gears in this paper. It is used to build a mathematical model, which achieves the auto judgment of the gear mesh state. We do not need to concern about active or passive gears any more, and the complicated power flow analysis can be avoided. With the numerical integration computation, the axis orbits diagram and dynamic gear mesh force characteristic are acquired and the results show that the dynamic response of translational displacement is greater when contacting line direction change is considered, and with the quickly change of direction of contacting line, the amplitude of mesh force would be increased, which easily causes the damage to the gear tooth. Moreover, compared with ordinary gear, dynamic responses of planetary gear would be affected greater by the gear backlash. Simulation results show the effectiveness of the generalized dynamic model and the mathematical model.

*Keywords:* geared system; the direction of contacting line; the variation of contacting line; generalized model; gear mesh force; axis orbits diagram.

### 1. Introduction

At present, it's a global challenge for human to improve traffic safety and reduce traffic accidents. The traffic accident is associated with the road environment, the state of the driver, and the condition of the vehicle<sup>[1-2]</sup>. Vehicle as the carrier of traffic safety, its status directly determines the safety of driver and

pedestrian. Geared systems are the most widely used power and motion transmission devices in various machines and mechanical equipments, whose mechanical behavior and performance have a critical impact on the entire machine<sup>[1-2]</sup>. With the increased demand for high speed machinery, mathematical modeling and dynamic analysis of gear drives gained importance<sup>[3]</sup>. Therefore, the geared system dynamics has been widely concerned

---

\* Corresponding : lh@bit.edu.cn.

over the past century, a lot of in-depth analyses and studies have made a considerable progress, and formed a complete theoretical system.

The vibration of geared system has been studied by many researchers (for example, see [4-17]). Daniel R. Kiracofe and Robert G. Parker extends previous analytical models of simple, single-stage planetary gears to compound, multi-stage planetary gears. This model is then used to investigate the structured vibration mode and natural frequency properties of compound planetary gears of general description, including those with equally spaced planets and diametrically opposed planet pairs<sup>[6]</sup>. Miroslav Byrtus and Vladimir Zeman presents an original method of the mathematical modeling of gear drive nonlinear vibrations using modal synthesis method with degrees of freedom number reduction<sup>[3]</sup>. Chen Siyu and Tang Jinyuan investigated the effects of the friction and backlash on the multi-degree of freedom nonlinear dynamic gear transmission system. The difference between the constant backlash and the dynamic backlash models is also discussed<sup>[8]</sup>. Cai-Wan and Chang-Jian performs a systematic analysis of the dynamic behavior of a gear-bearing system with nonlinear suspension, nonlinear oil-film force, and nonlinear gear mesh force. The dynamic orbits of the system are observed using bifurcation diagrams plotted with both the dimensionless unbalance coefficient and the dimensionless rotational speed ratio as control parameters<sup>[9]</sup>.

It is known that different simulation conditions determine the different directions and amplitudes of mesh forces. So it is generally requisite to complete the power flow analysis in order to determine the direction and formula of mesh force under a steady condition before dynamic modeling for a geared system. M Inalpolat and A Kahraman put forward the flowchart of the automatic transmission planetary gear dynamic modeling methodology which combined four different models<sup>[2]</sup> and the power flow analysis after kinematic analysis is necessary for geared system dynamic modeling in their researches.

In previous studies of gear dynamic modeling, the directions of gear mesh forces were always assumed unchanged under a steady condition, but during the actual gear meshing process, the direction of gear mesh force is more likely to change due to the vibration of gears. In this paper, firstly we define the gear mesh direction angle for

determining the variation and direction of contacting line of internal mesh and external mesh gears. Secondly, a generalized calculation formula is proposed to determine the variation of the contacting line, which can be appropriate for not only external mesh gears but also internal mesh gears. And a calculation formula of mesh force can be derived, which involves the direction and amplitude of the mesh force. Therefore the complicated power flow analysis is avoided, especially for complex geared systems including planetary gears. Thirdly, a generalized dynamic model of geared system is established, and it is possible to build a mathematical model which do not need to distinguish active gears from passive gears. Thus a complex geared system model can be built with the generalized model.

## 2. Modeling Theory

A generalized geared system dynamic model will be proposed in this section. Lagrange theorem and D'Alembert's principle are basic methods for building lumped mass dynamic models of geared systems. It is known that the model can be obtained by Lagrange theorem, which only needs a clear kinetic energy expression and a potential energy expression. In addition, it is necessary to finish the detailed mechanical analysis of nodes with D'Alembert's principle for building a geared system model. D'Alembert's principle is used to establish the generalized model in this paper. The flowchart of geared system dynamic modeling with generalized model is shown in Fig.1. This methodology combines as follows.

- (i) A kinematics formulation to compute the initial speeds and initial positions of the mesh gears, which will be used as the initial values during a numerical simulation.
- (ii) Generalized models of typical parts which are corresponding with nodes of the geared system model without power flow analysis.
- (iii) A complex geared system model based on these models of typical parts.
- (iv) Then the natural characteristic and dynamic response of a complex geared system can be achieved in the simulation.

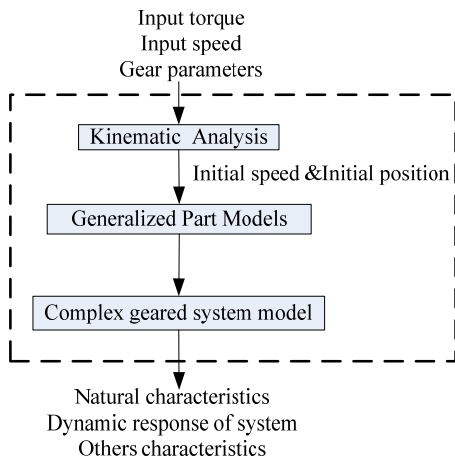


Fig.1. Flowchart of modeling for a geared system with a generalized dynamic model

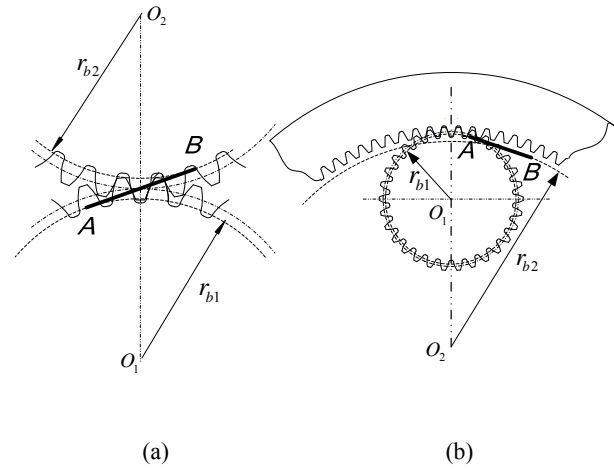


Fig. 2. Mesh line of external mesh gears and internal mesh gears

### 2.1. Variation and direction of the contacting line

It is known that the contacting line is defined as common tangent of two mesh gears. If two gears are external mesh gear, the contacting line is inner common tangent, such as line  $AB$  shown in Fig.2(a), if one of two gears is internal mesh gear, the contacting line is external common tangent, such as line  $AB$  shown in Fig.2(b). The dotted arcs present base circles of gears in Fig.2, and line  $AB$  is one of contacting lines. The position of the contacting lines indicates the direction of the mesh force, which determines the calculation formula of dynamic responses in translational directions.

In the following dynamic modeling research of geared systems, the gear mesh model uses a simplified representation by considering a linear spring along the contacting line of gears as shown in Fig.3(a). Firstly, determine the contacting line direction or position, then make the projection of the translational and torsional displacement on the contacting line to get the variation of the contacting line, and finally, the mesh force formula can be derived by multiplying the variation of contacting line with the mesh stiffness. So, the actual dynamics of geared system is strongly affected by correct description of the variation and direction of contacting line, especially for bending-torsional coupled vibration analysis. It is very necessary to study the variation and direction of the contacting line.

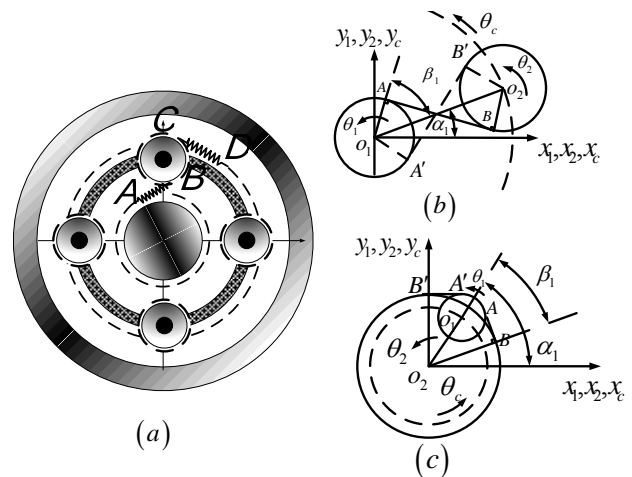


Fig. 3. Analysis of contacting line

Both the ordinary geared system and planetary geared system are widely used in many applications due to their advantages, such as high power density and large reduction in a volume. The ordinary geared system can be considered as a special form of a planetary geared system when the planet carrier is fixed. So we can take the planet carrier as a reference part for planetary geared system, just like taking the earth as reference for ordinary geared system. In order to build a generalized model, absolute Cartesian coordinates are introduced for each part. For planetary gear, the origin of coordinate will be set on the planet carrier geometric center, while the origin of coordinate will be set on their geometric centers for the sun gear, the ring gear and the planet carrier, which are also suitable for ordinary gears. Take the planetary gear

as an example shown in Fig.3(a), both external mesh gears and internal mesh gears involved in this system. In order to make a detailed analysis of contacting line, the planetary gear is abstracted into two parts as shown in Fig.3(b) and Fig.3(c).  $O_1$  represents the sun gear and  $O_2$  represents the planetary gear, while the dotted arc represents the planet carrier.  $AB$  and  $A'B'$  are two possible locations of contacting line as shown in Fig.3(b). First, take  $O_1$  as the origin of the Cartesian coordinates to establish  $(x_1, y_1, \theta_1)$ ,  $(x_2, y_2, \theta_2)$  and  $(x_c, y_c, \theta_c)$ , which indicate the translational and rotational displacement of two meshed gear and the planet carrier, then transfer the rotational and translational displacement to the direction of the contacting line in Fig.3(b). After analysis of the variance of contacting lines both at  $AB$  and  $A'B'$  direction, the formula of the contacting line variation for the external mesh gear can be derived as

$$\begin{aligned} \delta_1 = \text{sign}(\beta_1) & [(x_2 - R_{r2} \cos(\theta_c + \phi_2) - x_c - x_1) \\ & \sin(\theta_c + \alpha_1 + \beta_1) - (y_2 - R_{r2} \sin(\theta_c + \phi_2) \\ & - y_c - y_1) \cos(\theta_c + \alpha_1 + \beta_1) \\ & + (R_1(\theta_1 - \theta_c) + R_2(\theta_2 - \theta_c) + E)] \end{aligned} \quad (1)$$

$$\begin{aligned} \delta_2 = \text{sign}(\beta_2) & [(x_1 + x_c - x_2 + R_{r2} \cos(\theta_c + \phi_2)) \\ & \sin(\theta_c + \alpha_2 + \beta_2) - (y_1 + y_c - y_2 \\ & + R_{r2} \sin(\theta_c + \phi_2)) \cos(\theta_c + \alpha_2 + \beta_2) \\ & + (R_1(\theta_1 - \theta_c) + R_2(\theta_2 - \theta_c) + E)] \end{aligned} \quad (2)$$

Where  $\delta_1$ ,  $\delta_2$  represent the contacting line variations of gear 1 and gear 2;  $x_1, x_2, x_c, y_1, y_2, y_c$  are the translational displacements;  $\theta_1, \theta_2, \theta_c$  are the rotational displacements;  $\alpha_1$  is introduced as the initial angle from x-axis to vector  $\overline{O_1O_2}$ ,  $\alpha_2$  is introduced as the initial angle from x-axis to vector  $\overline{O_2O_1}$ , and  $\alpha_2 = \alpha_1 + \pi$ ;  $R_1, R_2$  are the base circle radius;  $R_{r1}, R_{r2}$  are the radius from geometric centers of two gears to geometric centers of planet carriers;  $\phi_1, \phi_2$  are the initial phases of two gears;  $E$  is the static transmission error which can be used to model the excitation due to profile modifications and manufacture errors;  $\beta_1, \beta_2$  are defined as the direction angles of contacting line, whose absolute values are equal to the pressure angles of mesh gears.

$$\beta_i = -\text{sign}[R_1(\theta_1 - \theta_c) + R_2(\theta_2 - \theta_c)]\alpha \quad i = 1, 2 \quad (3)$$

Where  $\alpha$  is the pressure angle of the mesh gear, which is generally equal to  $20^\circ$ .

As shown in Fig.3(c),  $O_1$  represents the planetary gear and  $O_2$  represents the ring gear, while the dotted arc represents the planet carrier,  $AB$  and  $A'B'$  are two possible locations of contacting line for internal mesh gear. Take  $O_2$  as the origin of the Cartesian coordinates to establish  $(x_1, y_1, \theta_1)$ ,  $(x_2, y_2, \theta_2)$  and  $(x_c, y_c, \theta_c)$ , which indicate the translational and rotational displacement of two meshed gear and the planet carrier, then transfer rotational and translational displacement to the direction of the contacting line in Fig.3(c). Similarly, the formula of the contacting line variation for the internal mesh gears can be derived as

$$\begin{aligned} \delta_1 = \text{sign}(\beta_1) & [(x_2 - x_1 + x_c + R_{r1} \cos(\theta_c + \phi_1)) \\ & \sin(\theta_c + \alpha_1 + \beta_1) - (y_2 - y_1 + y_c \\ & + R_{r1} \sin(\theta_c + \phi_1)) \cos(\theta_c + \alpha_1 + \beta_1) \\ & + (R_1(\theta_1 - \theta_c) - R_2(\theta_2 - \theta_c) + E)] \end{aligned} \quad (4)$$

$$\begin{aligned} \delta_2 = \text{sign}(\beta_2) & [(x_1 - R_{r1} \cos(\theta_c + \phi_1) \\ & - x_2 - x_c) \sin(\theta_c + \alpha_2 + \beta_2) - (y_1 - R_{r1} \sin(\theta_c + \phi_1) \\ & - y_2 - y_c) \cos(\theta_c + \alpha_2 + \beta_2) \\ & + (R_1(\theta_1 - \theta_c) - R_2(\theta_2 - \theta_c) + E)] \end{aligned} \quad (5)$$

where  $\beta_1, \beta_2$  are defined as the direction angles of contacting line whose absolute values are individually equal to the pressure angles of mesh gears

$$\beta_i = -\text{sign}[R_1(\theta_1 - \theta_c) - R_2(\theta_2 - \theta_c)]\alpha \quad i = 1, 2 \quad (6)$$

A generalized formula for describing the variation of contacting line is derived from Eqs (1)-(6), which is suitable for both the external mesh gear and the internal mesh gear

$$\begin{aligned}
 \delta_i = & \text{sign}(\beta_i)[(x_j - R_{rj} \cos(\theta_c + \phi_j) \\
 & -x_i + R_{ri} \cos(\theta_c + \phi_i) + x_c(\text{sign}(R_{ri}) \\
 & -\text{sign}(R_{rj}))\sin(\theta_c + \alpha_i + \beta_i) \\
 & -(y_j - R_{rj} \sin(\theta_c + \phi_j) - y_i \\
 & + R_{ri} \sin(\theta_c + \phi_i) + y_c(\text{sign}(R_{ri}) \\
 & -\text{sign}(R_{rj}))\cos(\theta_c + \alpha_i + \beta_i)) \\
 & +(\text{sign}(\gamma_i)R_i(\theta_i - \theta_c) + \text{sign}(\gamma_j)R_j(\theta_j - \theta_c) + E)]
 \end{aligned} \tag{7}$$

Where  $\delta_i$  represents the variation of contacting line, which is suitable for both external mesh gear and internal mesh gear;  $x_i, x_j, x_c, y_i, y_j, y_c$  are the translational displacements;  $\theta_i, \theta_j, \theta_c$  are the rotational displacements;  $\alpha_i$  is introduced as the initial angle from x-axis to vector  $\overline{O_i O_j}$ ,  $\alpha_j$  is introduced as the initial angle from x-axis to vector  $\overline{O_j O_i}$ , and  $\alpha_j = \alpha_i + \pi$ ;  $R_i, R_j$  are the base circle radius;  $R_{ri}, R_{rj}$  are the radius from the geometric centers of two gears to the centers of planet carriers;  $\phi_i, \phi_j$  are the initial phases of two gears;  $E$  is the static transmission error which can be used to model excitation due to the profile modifications and the manufacture errors;  $\gamma_i$  is introduced to distinguish the gear mesh types, if gear  $i$  is an external mesh gear then  $\gamma_i = 1$ , else if gear  $i$  is an internal mesh gear then  $\gamma_i = -1$ ;  $\beta_i$  is defined as the direction angle of contacting line whose absolute value is equal to the pressure angle of mesh gears

$$\beta_i = -\text{sign}[\text{sign}(\gamma_i)R_i(\theta_i - \theta_c) + \text{sign}(\gamma_j)R_j(\theta_j - \theta_c)]\alpha \tag{8}$$

An ordinary geared system can be seen as a special form of a planetary geared system when the planet carrier is fixed. So for an ordinary geared system, Eqs. (7) can be simplified as

$$\begin{aligned}
 \delta_i = & \text{sign}(\gamma_j \beta_i)[(x_j - x_i)\sin(\alpha_i + \beta_i) \\
 & -(y_j - y_i)\cos(\alpha_i + \beta_i) + \text{sign}(\gamma_i)R_i\theta_i \\
 & + \text{sign}(\gamma_j)R_j\theta_j + E]
 \end{aligned} \tag{9}$$

$$\beta_i = -\text{sign}[\text{sign}(\gamma_i)R_i\theta_i + \text{sign}(\gamma_j)R_j\theta_j]\alpha \tag{10}$$

## 2.2. Establishment of the generalized model

It is necessary to make the detailed mechanical analysis of nodes with D'Alembert's principle to establish the generalized model of a geared system. For a node with bending-torsional coupled degrees of freedom, the loads acted on the node can be as the inertial force, the inertia moment, the elastic bending force and elastic torsional torque of the shaft, the bearing reaction force, the gear mesh force, external forces and moments, etc. A detailed mechanical analysis is shown in the following section.

### 2.2.1. Inertial force and inertia moment

$$\begin{cases}
 F_{ax} = ma_{cx} \\
 F_{ay} = ma_{cy} \\
 T_a = (J + me^2)\ddot{\theta}_i - F_{ax}e_i \sin(\theta_i + \psi_i) \\
 \quad + F_{ay}e_i \cos(\theta_i + \psi_i)
 \end{cases}$$

Where  $F_{ax}, F_{ay}$  are the inertial forces in  $x$  and  $y$  directions,  $T_a$  is the inertial moment in the torsional direction;  $m$  is the mass of the node,  $J$  is the polar mass moment of inertia, and  $e$  is the eccentricity of the node,  $a_{cx}, a_{cy}$  are the centroid accelerations in  $x$  and  $y$  directions,  $\theta_i, \dot{\theta}_i$  are the torsional displacement and torsional acceleration,  $\psi_i$  is the initial angle of eccentricity.

### 2.2.2. Elastic bending force and torque of shaft

$$\begin{cases}
 F_{sx} = K(l, :)X + C(l, :)\dot{X} \\
 F_{sy} = K(l, :)Y + C(l, :)\dot{Y} \\
 T_s = -F_{sx}R_{ri} \sin(\theta_i + \phi_i) + F_{sy}R_{ri} \cos(\theta_i + \phi_i)
 \end{cases}$$

Where  $F_{sx}, F_{sy}$  are the elastic bending forces of shaft in  $x$  and  $y$  directions,  $T_s$  is the torque caused by the elastic bending force of shaft.  $X = [x_1, x_2, \dots, x_l, \dots, x_n]^T$  is  $x$  displacement vector, as the shaft is discrete into  $n$  nodes,  $Y = [y_1, y_2, \dots, y_l, \dots, y_n]^T$  is  $y$  displacement vector,  $i$  is the node number of one part, while  $l$  is the arrange number of node  $i$  on shaft.  $\dot{X}, \dot{Y}$  are the derivatives of  $X$  and  $Y$ .  $\theta_i$  is the torsional displacement of node  $i$ .  $\phi_i$  is the initial phase of node  $i$ .  $K(l, :)$  is the  $l$ -th row vector

of the bending stiffness matrix of shaft,  $C(l,:)$  is the  $l$ -th row vector of the bending damping matrix of shaft.

### 2.2.3. Elastic torsional torque of shaft

$$T_i = \sum [k_{ij}(\theta_i - \theta_j) + c_{ij}(\dot{\theta}_i - \dot{\theta}_j)]$$

Where  $T_i$  are the elastic torsional torque of shaft,  $k_{ij}$ ,  $c_{ij}$  are torsional stiffness and damping of shaft from node  $i$  to node  $j$ ,  $\theta_i, \theta_j$  are torsional displacements of node  $i$  and node  $j$ ,  $\dot{\theta}_i, \dot{\theta}_j$  are torsional velocities of node  $i$  and node  $j$ .

### 2.2.4. Bearing reaction force and torque

Bearings are widely used in geared systems, there are two main types of the bearing support: fixed support and floating support. The locations of two parts supported by fixed bearing are fixed, for instance ball bearings are used to support the ordinary gear. At least one of two parts supported by floating bearing has a planetary gear revolution movement, for instance the needle bearing which is used to support the planetary gear and planet carrier.

If there is a planetary gear revolution for node  $i$ , such as planetary gear, the needle bearing reaction forces are expressed as

$$\begin{cases} F_{bx} = k_{bx}(x_i - x_j - R_{ri} \cos(\theta_j + \phi_i)) \\ + c_{bx}(\dot{x}_i - \dot{x}_j + R_{ri} \dot{\theta}_j \sin(\theta_j + \phi_i)) \\ F_{by} = k_{by}(y_i - y_j - R_{ri} \sin(\theta_j + \phi_i)) \\ + c_{by}(\dot{y}_i - \dot{y}_j - R_{ri} \dot{\theta}_j \cos(\theta_j + \phi_i)) \\ T_b = 0 \end{cases}$$

Where  $F_{bx}$ ,  $F_{by}$  are the bearing reaction forces,  $T_b$  is the bearing torque caused by the bearing reaction force, and its amplitude is zero because the bearing reaction force was imposed on the geometric center of node  $i$ .  $k_{bx}, k_{by}, c_{bx}, c_{by}$  are the reaction stiffness and damping of bearings in x-direction and y-direction.  $x_i, x_j, y_i, y_j$  are the translational displacements of node  $i$  and  $j$  in x and y directions, while  $\dot{x}_i, \dot{x}_j, \dot{y}_i, \dot{y}_j$  are the translational velocities of node  $i$  and  $j$  in x and y directions.  $R_{ri}$  is the revolution radius of node  $i$  relative to node  $j$ .  $\theta_j, \dot{\theta}_j$  are

the torsional displacement and rotational velocity of node  $i$ .  $\phi_i$  is the initial phase of node  $i$ .

If there is a planetary gear revolution for node  $j$ , which revolves along node  $i$ . Node  $i$  can be considered as planet carrier. For node  $i$ , the bearing reaction forces can be expressed as

$$\begin{cases} F_{bx} = k_{bx}(x_i + R_{rj} \cos(\theta_i + \phi_j) - x_j) \\ + c_{bx}(\dot{x}_i - R_{rj} \dot{\theta}_i \sin(\theta_i + \phi_j) - \dot{x}_j) \\ F_{by} = k_{by}(y_i + R_{rj} \sin(\theta_i + \phi_j) - y_j) \\ + c_{by}(\dot{y}_i + R_{rj} \dot{\theta}_i \cos(\theta_i + \phi_j) - \dot{y}_j) \\ T_b = -F_{bx} R_{rj} \sin(\theta_i + \phi_j) + F_{by} R_{rj} \cos(\theta_i + \phi_j) \end{cases}$$

Where  $F_{ax}$ ,  $F_{ay}$  are the bearing reaction forces,  $T_b$  is the bearing torque caused by the bearing reaction force and its amplitude is non-zero, because the bearing reaction force is imposed on the center of circle with radius  $R_{rj}$  from the center of the node  $i$ .  $R_{rj}$  is the revolution radius of node  $j$  relative to node  $i$ .  $k_{bx}, k_{by}, c_{bx}, c_{by}$  are the reaction stiffness and damping of bearing in x-direction and y-direction.  $x_i, x_j, y_i, y_j$  are the translational displacements of node  $i$  and  $j$  in x and y directions, while  $\dot{x}_i, \dot{x}_j, \dot{y}_i, \dot{y}_j$  are the translational velocities of node  $i$  and  $j$  in x and y directions.  $\theta_j, \dot{\theta}_j$  are the torsional displacement and rotational velocity of node  $i$ .  $\phi_j$  is the initial phase of node  $j$ .

If node  $i$  is supported by fixed support bearing, the bearing reaction forces can be expressed as

$$\begin{cases} F_{bx} = k_{bx}(x_i - x_j) + c_{bx}(\dot{x}_i - \dot{x}_j) \\ F_{by} = k_{by}(y_i - y_j) + c_{by}(\dot{y}_i - \dot{y}_j) \\ T_b = 0 \end{cases}$$

Where  $F_{bx}$ ,  $F_{by}$  are the bearing reaction forces,  $T_b$  is the bearing torque caused by the bearing reaction force, its amplitude is zero because the bearing reaction force imposed on the center of the node  $i$ .  $k_{bx}, k_{by}, c_{bx}, c_{by}$  are the reaction stiffness and damping of bearing in x-direction and y-direction.  $x_i, x_j, y_i, y_j$  are the translational displacements of node  $i$  and  $j$  in x and y directions, while  $\dot{x}_i, \dot{x}_j, \dot{y}_i, \dot{y}_j$  are the translational velocities of node  $i$  and  $j$  in x and y directions.

There may be many bearings for one node, such as planet carrier, where there are at least three needle bearings or more. So all bearing reaction forces must be considered during geared system modeling.

2.2.5. Gear mesh force and torque

$$\begin{cases} F_{mx} = \sum [-\text{sign}(\beta_i)(k_m \delta_i + c_m \dot{\delta}_i) \sin(\theta_c + \alpha_i + \beta_i)] \\ F_{my} = \sum [\text{sign}(\beta_i)(k_m \delta_i + c_m \dot{\delta}_i) \cos(\theta_c + \alpha_i + \beta_i)] \\ T_m = \sum [\text{sign}(\beta_i)(k_m \delta_i + c_m \dot{\delta}_i) R_i] \end{cases}$$

Where  $F_{mx}$ ,  $F_{my}$  are the gear mesh forces of node  $i$  in x-direction and y-direction.  $T_m$  is the torque caused by the gear mesh force.  $k_m, c_m$  are individually the mesh stiffness and the mesh damping.  $\delta_i, \dot{\delta}_i$  are the variation of the contacting line and its derivative.  $\theta_c$  is the torsional displacement of the planet carrier, and it is equal to zero for node  $i$  if node  $i$  is an ordinary gear.  $\alpha_i$  is the initial angle of node  $i$ .  $\beta_i$  is defined as the direction angle of the contacting line.  $R_i$  is the base circle radius. The mesh force formula will be non-linear if we consider of the time-varying mesh stiffness and the gear backlash<sup>[3]</sup>. In the following application sample, the backlash function can be described as:

$$f(\delta, b) = \begin{cases} \delta - b & \delta \geq b \\ 0 & -b < \delta < b \\ \delta + b & \delta \leq -b \end{cases}$$

Where  $f(\delta, b)$  is backlash function,  $\delta$  is the variation of the contacting line,  $b$  is the backlash of gear.

The generalized dynamic model for a geared system can be derived by above mechanical analysis.

$$\begin{cases} F_{ax} + F_{sx} + F_{bx} + F_{mx} = F_x(t) \\ F_{ay} + F_{sy} + F_{by} + F_{my} = F_y(t) \\ T_a + T_s + T_b + T_t + T_m = T(t) \end{cases} \quad (11)$$

Where  $F_{ax}, F_{ay}, T_a$  are the inertial forces and inertia moment,  $F_{sx}, F_{sy}$  are the elastic bending forces of shaft,  $T_s$  is the torque caused by the elastic bending force of shaft,  $F_{bx}, F_{by}$  are the bearing reaction forces,  $T_b$  is the torque caused by the bearing reaction force,  $F_{mx}$  and  $F_{my}$  are the mesh forces,  $T_m$  is the torque caused by the gear mesh

force,  $T_m$  is the elastic torsional torque of shaft,  $F_x(t)$  and  $F_y(t)$  are the external forces,  $T(t)$  is the external moment.

The generalized model of a geared system can be changed into different kinds of models, such as a pure torsional linear model, a pure torsional nonlinear model, a bending-torsional coupled linear model.

The variation and direction of contacting line can be clearly given by Eqs. (7)-(10), and the mesh force formula can be derived by multiplying the variation of contacting line with the mesh stiffness. Then the generalized geared system dynamic model can help to build a mathematical model which do not need to distinguish the active gears from the passive gears, so the complicated power flow analysis, especially for complex systems such as planetary drive would be avoided.

3. Application of the Generalized Model

The drive system is shown in Fig.4 which is used to verify the validity of the generalized model.

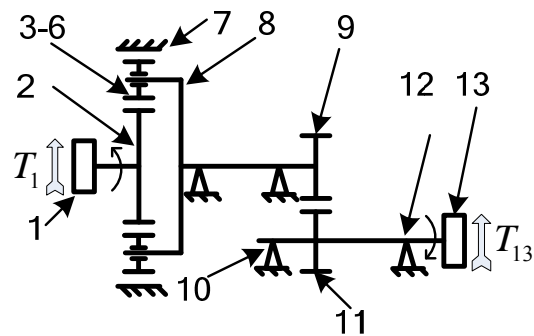


Fig. 4. Transmission diagram

Both ordinary gears and planetary gears are included in this geared system as shown in Fig.4. Node 1 and node 13 are respectively the input and output inertia disk. Node 2 is the sun gear, node 3-6 are the planetary gears, node 7 is the ring gear, node 8 is the planet carrier, both node 9 and node 11 are the ordinary gears. There are four fixed bearing supports and four floating supports as shown in Fig.4. Node 1 and node 2 are considered as pure torsional nodes, node 7 is the fixed node, the other nodes are bending-torsional coupled nodes, node 8 and node 9 are supported by fixed bearings, node 10 and node 12 are fixed bearings.

3.1. The major parameters of the system

There are 33 degrees of freedom in this model as shown in Table 1, which also shows the mechanical

analysis of all nodes of system. The major parameters of this geared system are shown in Table 2.

Table 1. Degrees of freedom and mechanical analysis of the example system shown in Fig.2.

Nodes	Degrees of freedom			Mechanical analysis				
	<i>x</i>	<i>y</i>	$\theta$	$F_{ax}, F_{ay}, T_a$	$F_{sx}, F_{sy}, T_s$	$T_t$	$F_{bx}, F_{by}, T_b$	$F_{mx}, F_{my}, T_m$
1			✓	$T_a$		$T_t$		
2			✓	$T_a$		$T_t$		$T_m$
3~6	✓	✓	✓	$F_{ax}, F_{ay}, T_a$			$F_{bx}, F_{by}$	$F_{mx}, F_{my}, T_m$
7			✓	$T_a$				$T_m$
8	✓	✓	✓	$F_{ax}, F_{ay}, T_a$	$F_{sx}, F_{sy}, T_s$	$T_t$	$F_{bx}, F_{by}, T_b$	$F_{mx}, F_{my}, T_m$
9	✓	✓	✓	$F_{ax}, F_{ay}, T_a$	$F_{sx}, F_{sy}, T_s$	$T_t$	$F_{bx}, F_{by}$	$F_{mx}, F_{my}, T_m$
10	✓	✓	✓	$F_{ax}, F_{ay}, T_a$	$F_{sx}, F_{sy}, T_s$	$T_t$	$F_{bx}, F_{by}$	
11	✓	✓	✓	$F_{ax}, F_{ay}, T_a$	$F_{sx}, F_{sy}, T_s$	$T_t$		$F_{mx}, F_{my}, T_m$
12	✓	✓	✓	$F_{ax}, F_{ay}, T_a$	$F_{sx}, F_{sy}, T_s$	$T_t$	$F_{bx}, F_{by}$	
13	✓	✓	✓	$F_{ax}, F_{ay}, T_a$	$F_{sx}, F_{sy}, T_s$	$T_t$		

Table 2. Parameters of the example system shown in Fig.2

Mass(kg)	$m_1=2, m_2=2.6779, m_3=m_4=m_5=m_6=0.5208112, m_7=0.5208, m_8=7.568, m_9=2.83408, m_{10}=1.15, m_{11}=3.8637, m_{12}=1.15, m_{13}=2$
Mass moment of inertia(kg · m <sup>2</sup> )	$J_1=0.0044, J_2=0.00369818, J_3=J_4=J_5=J_6=0.000200525, J_7=0.000200525, J_8=0.0156, J_9=0.00413958, J_{10}=0.002, J_{11}=0.00767244, J_{12}=0.002, J_{13}=0.0044$
Module and number of teeth	$m_n=3\text{mm}; z_2=35, z_3=z_4=z_5=z_6=17, z_7=69, z_9=36, z_{11}=42$
Mesh stiffnesses(N/m)	$k_{m23}=k_{m24}=k_{m25}=k_{m26}=k_{m37}=k_{m47}=k_{m57}=k_{m67}=k_{m911}=5.8e8$
Gear backlash(mm)	$b_{23}=b_{24}=b_{25}=b_{26}=b_{37}=b_{47}=b_{57}=b_{67}=b_{911}=0.200$
Bearing stiffnesses(N/m)	$k_{b3}=k_{b4}=k_{b5}=k_{b6}=1.55e8, k_{b8}=k_{b9}=1.53e8, k_{b10}=k_{b12}=1.53e8$
Torsional stiffnesses(Nm/rad)	$k_{1,2}=394488.78, k_{8,9}=2366932.69, k_{10,11}=10144083.62, k_{11,12}=6238611.42, k_{12,13}=12997107.13$
Bending stiffness matrices**(N/m)	$K_1 = \begin{bmatrix} 160261067.93 & -160261067.93 \\ -160261067.93 & 160261067.93 \end{bmatrix}, K_2 = \begin{bmatrix} 1112114942.39 & -2027130054.11 & 1396399324.54 & -481384212.82 \\ -2027130054.11 & 4105982000.55 & -3812533119.69 & 1733681173.25 \\ 1396399324.54 & -3812533119.69 & 5660609233.81 & -3244475438.66 \\ -481384212.82 & 1733681173.25 & -3244475438.66 & 1992178478.23 \end{bmatrix}$
External moments(Nm)	$T_1=1000, T_{13}=3466.67$

\*\* Note:  $K_1$  is bending stiffness matrix of shaft including node 8 and node 9.  $K_2$  is bending stiffness matrix of shaft including node 10, node 11, node 12 and node 13.

3.2. Results

The ring gear is fixed as shown in Fig.4. The input rotational speed is 4200 r/min, the input torque acted on node 1 is 1000Nm and the resistance moment acted on node 13 is 3466.67Nm. After the numerical simulation with the fourth-order Runge-Kutta method, the solution results without damping are shown as follows.

3.2.1. Axis orbits diagram

Axis orbit diagram is one of phase diagrams, which plots the position of the objects. According to the

theoretical analysis, the axis orbit is predictable for some nodes, which can be used to show the effectiveness of the model.

If the contacting line direction is unchangeable for all gears in a steady condition simulation, the direction of the gear mesh force is also unchangeable. The carrier is imposed on the reaction forces of four needle bearing whose vector sum is equal to zero. So the axis orbit of planet carrier is mostly influenced by the direction of the gear mesh force of node 9. The theoretical axis orbit of carrier should be a straight line with expression  $y = \tan(70 * \pi / 180) * x$ . Axis orbit of planet carrier with unchangeable contacting line direction for

all gears is shown in Fig.5. It is clearly that the axis orbit diagram of planet carrier is corresponding to it.

It is assumed that the contacting line direction is changeable for all gears in a stable simulation on vibration and shock of gears, which is clearly more similar to the practical situation. Axis orbit of planet carrier with changeable contacting line direction for all gears is shown in Fig.6. The simulation curves dramatically fluctuate roughly along with the theoretical line, which is introduced by the reverse impact of gears.

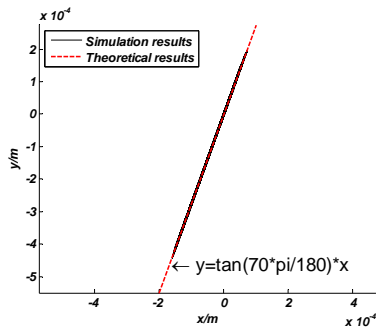


Fig. 5. Axis orbit of planet carrier with unchangeable contacting line direction for all gears

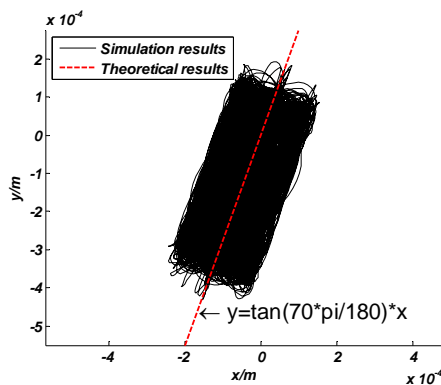


Fig. 6. Axis orbit of planet carrier with changeable contacting line direction for all gears

For planetary gears, absolute Cartesian coordinates are fixed on the point coincided with the planet carrier geometric center, so the planetary axis orbit is a circle with a radius of 0.078m. The dynamic response of the planetary gear is consistent with the theoretical analysis as shown in Fig.7.

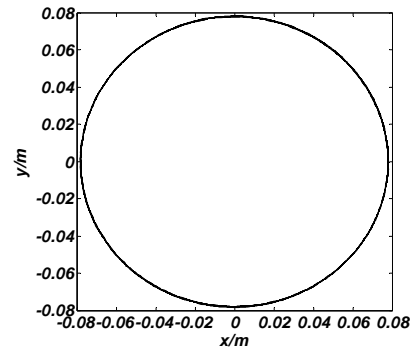


Fig. 7. Axis orbit of planetary gear with changeable contacting line direction for all gears

From Fig.5-Fig.7, the axis orbits or the translational displacements of nodes are strongly influenced by the direction of contacting lines, which also indicates the direction of mesh force. Compared with Fig.5, Fig.6 shows that the responses of translational displacement when considering the changes of the direction of contacting line are greater than that not considered. On the other hand, simulation results also prove the validity of the generalized model.

### 3.2.2. Dynamic mesh force response

Node 3 is a planetary gear. The relation between mesh force and direction angle of contacting line of node 3 is shown in Fig.8~Fig.11. The theoretical direction angle of the contacting line of node 3 is  $-20^\circ$  for the external mesh gear and  $20^\circ$  for the internal mesh gear. Fig.8 and Fig.10 show that if we do not consider the direction changes of the contacting line, there is no obvious impact force during the process of power flowing through the geared system. On the contrary, if we consider the direction changes of contacting line, as shown in Fig.9, the alternating changes from  $-20^\circ$  to  $20^\circ$  of contacting line direction for the external mesh gear will occur because of the impact of mesh gear during power flowing through geared system, while the direction of the contacting line for the internal mesh gear changes from  $20^\circ$  to  $-20^\circ$  as shown in Fig.11. At the time range of 0.05~0.07s as shown in Fig.9 and Fig.11, the impacts of gears occur frequently, which can be explained by the angle of the contacting line. The contacting line angle changes more frequently, the amplitude for mesh force will be greater, which easily causes damage to the gear tooth. The mesh

forces of both the external mesh gear and the internal mesh gear when considering the changes of contacting line reach peaks almost at the same time, when the simulation time is about 0.06s, the maximum dynamic load coefficients are 18.77 for the external mesh gears and 18.81 for the internal mesh gear, while the maximum dynamic load coefficients are only 2.23 for the external mesh gear and 2.31 for the internal mesh gear if we do not consider the change of the contacting line direction. So the changes of the contacting line direction have an important influence on dynamic response of the geared system and that must be considered in the modeling of geared system, especially for the bending-torsional coupled model.

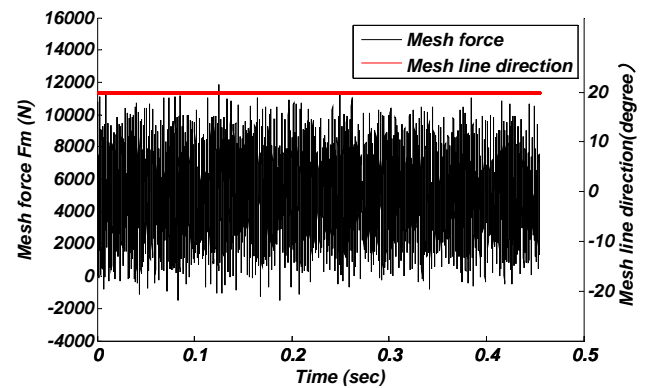


Fig. 10. Internal mesh force and contacting line direction of node 3 with unchangeable contacting line direction for all gears

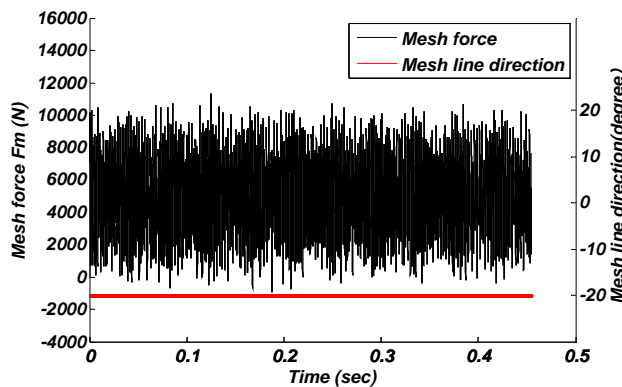


Fig. 8. External mesh force and contacting line direction of node 3 with unchangeable contacting line direction for all gears

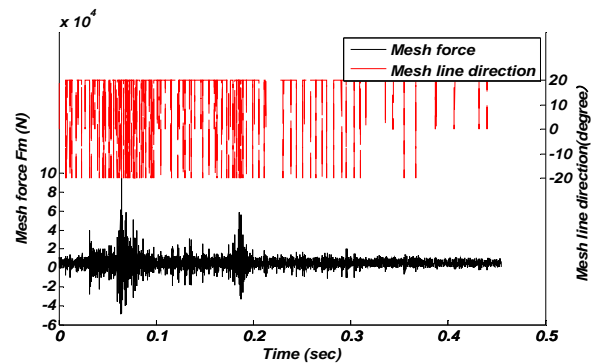


Fig. 11. Internal mesh force and contacting line direction of node 3 with changeable contacting line direction for all gears

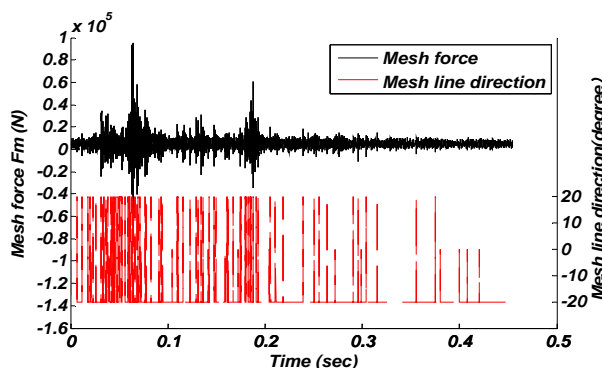


Fig. 9. External mesh force and contacting line direction of node 3 with changeable contacting line direction for all gears

The relation between the mesh force and the direction angle of contacting line for node 11 is shown in Fig.12 and Fig.13. Node 11 is an ordinary gear. Compared with Fig.12, Fig.13 shows that reverse impact forces will be caused for mesh gear under the impact of power flowing through geared system. The maximum dynamic load coefficient is 1.92 for node 11 if we consider the changes of contacting line as shown in Fig.13, while the maximum dynamic load coefficient is 1.83 for node 11 if we do not consider of contacting line changes as shown in Fig.12. The gear backlash has a greater impact on dynamic response of the planetary gear than that of the ordinary gear compared with the maximum dynamic load coefficients, which changes over eight times under two conditions: the changes of contacting line are considered conditions or not.

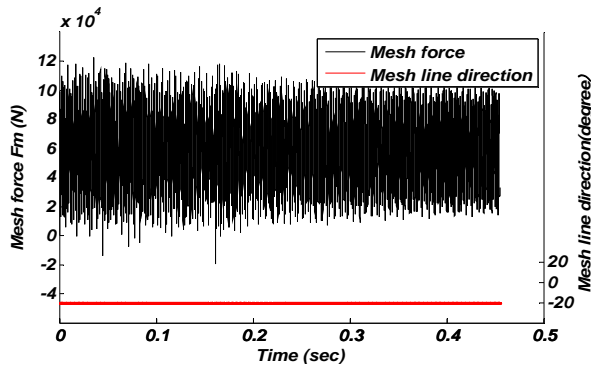


Fig.12. Mesh force of node 11 with unchangeable contacting line direction for all gears

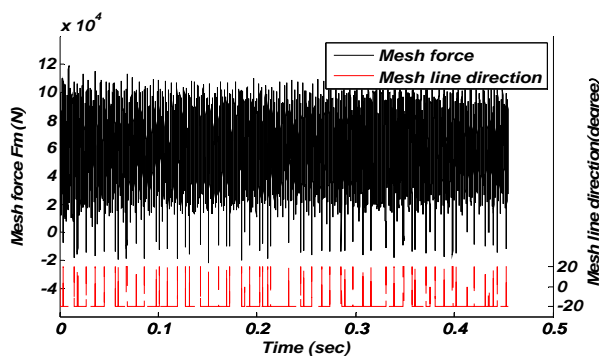


Fig. 13. Mesh force of node 11 with changeable contacting line direction for all gears

**4. Conclusions**

- (i) The formula of the contacting line variation is derived by the introduced definition of the direction angle of contacting line, and it becomes possible not to distinguish the internal mesh gear from the external mesh gear. It establishes the foundation for the derivation of the generalized model of a geared system.
- (ii) According to the analyses of the variation and direction of the contacting line for the internal mesh gear and external mesh gear, the generalized dynamic model of a geared system is established. The dynamic model can help to build a mathematical model, and do not need to distinguish active gears from passive gears, so complicated power flow analysis, especially for complex systems including planetary gears will be avoided which will greatly improve the efficiency of modeling .

- (iii) The mathematical model of a geared system including both the ordinary gears and the planetary gears is established with the generalized model. Through the consideration of the unchangeable and changeable contacting line direction, the validity and applicability of the generalized model is verified based on the dynamic analysis. The impact response of the geared system caused by the change of contacting line direction angle is researched. The contacting line angle changes more frequently, the amplitude of the mesh force will be greater, which easily causes the damage to the gear tooth. The gear backlash has a greater impact on the dynamic response of the planetary gear than that on the ordinary gear.
- (iv) In the future study, the generalized model also can be used to build the model of a system with a double-planet set or a complex-compound gear set. The generalized model can be further used to automatically build the model of a geared system to meet different transmission routes for different shifts in the gear shifting process.

**5. Acknowledgements**

This work was partially supported by Natural Nature Science Foundation of China (50905018, 51075033). The authors would like to express gratitude to its financial support.

**References**

1. Wuhong Wang,Xiaobei Jiang,Shuangcheng Xia,Qi Cao.Incident tree model and incident tree analysis method for quantified risk assessment:an in-depth accident study in traffic operation,*Safety Science*, 48(10) (2010),1248-1262
2. Wuhong Wang,Yan Mao,Jin Jing,Xiao Wang,Hongwei Guo,Xuemei Ren,Ikeuchi Katsushi,Driver’s various information process and multi-ruled decision-making mechanism:a fundamental of intelligent driving shaping model,*International Journal of Computational Intelligence System* , 4(3) (2011),297-305
3. M Inalpolat, A Kahraman.Dynamic modelling of planetary gear of automatic transmissions.*Proc. ImechE*, 222(2008):229-242
4. LI Run-fang, WANG Jian-jun.Gear System Dynamics - Vibration, Impact, *Noise.Science Press*, 1997
5. Smith,J.D.Gears and their vibration:A basic approach to understanding gear noise,*Marcel-Dekker,inc*,1993
6. WANG Jianjun,LI Runfang,PENG Xianghe.Survey of nonlinear vibration of gear transmission systems,*Journal of Applied Mechanical* , 56(3) (2003),:309-329

7. KAHRAMAN,A.BLANKENSHIP G W. Experiments on nonlinear dynamic behavior of an oscillator with clearance and periodically time-varying parameters.*Journal of Applied Mechanics*, 64(1997): 217-226
8. Daniel R.Kiracofe,Robert G..Parker.Structured vibration modes of general compound planetary.*Journal of vibraton and acoustics*, 129(2007):1-16
9. Miroslav Byrtus,Vladimir Zeman.On modeling and vibration of gear drives influenced by nonlinear couplings.*Mechanism and Machine Theory* 46(2011) 375-397
10. Chen Siyu,Tang Jinyuan,Luo Caiwang,Wang Qibo.Nonlinear dynamic characteristics of geared rotor bearing systems with dynamic backlash and friction. *Mechanism and Machine Theory* 46(2011) 466-478
11. Cai-Wan,Chang-Jian.Strong nonlinearity analysis for gear-bearing system under nonlinear suspension-bifurcation and chaos.*Nonlinear Analysis:Real Word Applications* 11(2010) 1760-1774
12. LI Ming, SUN Tao, HU Haiyan. Review on dynamic of geared rotor-bearing systems.*Journal of vibration engineering*, 15(3) (2002):249-256
13. WANG Xiaosun, WU Shijing, ZHOU Xuhui, LI Qunli. Bifurcation and chaos in a nonlinear dynamic model of spur gear with backlash. *Journal of vibration and shock*, 27(1)(2008):53-56
14. SHEN Yongjun,YANG Shaopu,PAN Cunzhi,XING Haijun. Nolinear dynamics of a spur gear pair to parametric and external excitation.*Journal of Beijing jiaotong university*, 29(1) (2005):69-73
15. LIU Xiaoning, WANG Sanmin, SHEN Yunwen.Nonlinear Vibrations of 3-DOF Geared Rotor-Bearing System.*Mechanical science and technology*, 23(10) (2004):1191-1193
16. SUN Tiantian. Bending-Torsional Coupled Vibration Characteristics Analysis of Vehicle Powertrain, *PHD Thesis at Beijing Institute of Technology*, Beijing , P.R.China,2009
17. Cheon-Jae Bahk, Robert G. Parker.Analytical Solution for the Nonlinear Dynamics of Planetary Gears. *Journal of Computational and Nonlinear Dynamics*, 6(4) (2011):021007-1-021007-15